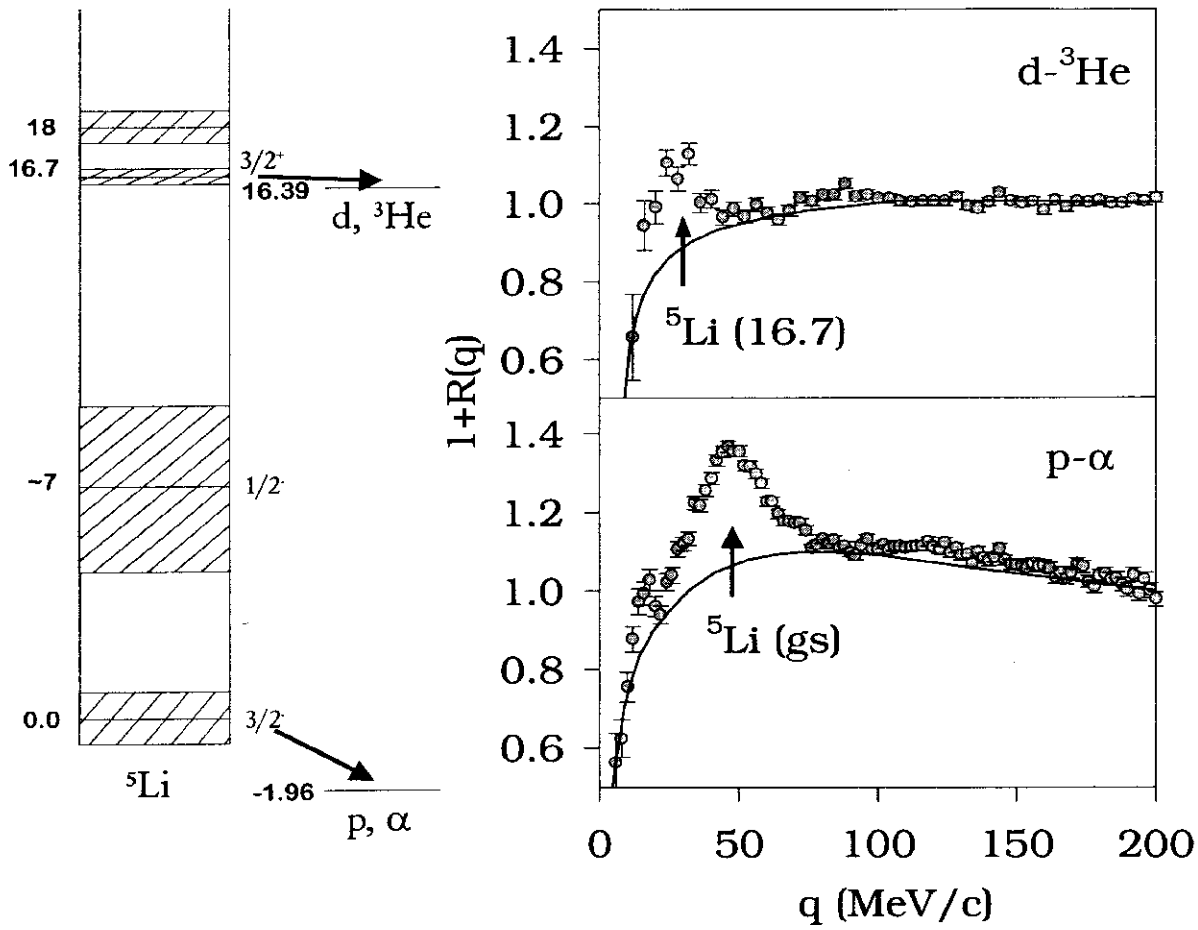

Experimental correlation functions for p - α (bottom panel) and d - ^{3}He coincidences (top panel), as function of the momentum of relative motion q between the coincident particles, for the reaction Au + Au at 150 MeV per nucleon. The figure illustrates that resonances from the decay of the ground and excited (16.7 MeV) states of ^{5}Li are observed in these channels (indicated by the arrows). The technique of correlation functions is used in order to extract the production yields for these resonances. From their ratio, weighted with the channel spin factors, emission temperatures can be determined.

Investigating Temperature and Space-Time Behaviour of Fragment Formation

Introduction

A new method to determine emission temperatures in nuclear reactions, based on double ratios of isotopic yields, was recently developed. The obtained temperatures, plotted against the measured excitation energies of the decaying systems, allowed us to deduce a caloric curve of nuclei [1, 2]. Here, the new data at high excitation energies up to 15 MeV per nucleon were derived for excited spectator systems produced in Au + Au collisions at a bombarding energy of 600 MeV per nucleon. Previous experiments had shown that, in this range of relativistic energies, the decay of excited spectators proceeds independently of the entrance channel dynamics and without indications of collective outward flow [3]. Therefore, projectile spectators, which are produced over a wide range of excitation energy and mass in these reactions, are well suited for the investigation of highly excited nuclear systems in thermodynamical equilibrium.

The observed S-shaped behaviour of the caloric curve of nuclei is reminiscent of a first-order phase transition in macroscopic systems. A region of constant temperature of T $\approx$ 5 MeV separates the 'liquid' and 'vapour' regimes where the temperature rises with increasing excitation energy. In particular, the recent observation of the rise of the emission temperature at excitation energies exceeding 10 MeV per nucleon has initiated a widespread discussion of these data which addresses both, methodical aspects and questions of interpretation [5, 6, 7].

There is an obvious need for new data, in fact independent of the actual status of the present discussion. A large part of the temperature measurements which are presently available in the literature have been obtained by measuring the yields of particle-unstable states in correlation experiments [8, 9, 10, 11, 12, 13]. From the ratios of yields of excited states in the same isotope the temperatures are deduced by applying the Boltzmann factor. The use of this method in an exclusive measurement of the same reaction will permit a crosscomparison of two different 'thermometers' which is mandatory for the quantitative interpretation of the results. Furthermore, the fragment formation in reactions exhibiting rapid expansion due to collective radial flow is of particular interest presently [3, 4, 14, 15, 16, 17]. The investigation of this phenomenon and its possible relation to the liquid-gas phase transition in nuclei requires experimental knowledge on emission temperatures and the space-time behaviour.

The new series of experiments was performed during spring of 1995. Collisions of Au + Au were studied at two regimes of bombarding energies: 1 GeV per nucleon in order to continue on the investigation of spectator decays following peripheral and mid-central collisions, and at 50, 100, 150, and 200 MeV per nucleon in order to examine central reactions which are known to exhibit a considerable collective flow.

Experimental method

The experiment was performed at the ALADIN spectrometer. A schematic view of the experimental setup is shown in Fig. 1. Three hodoscopes, provided by GSI, MSU, and LNS Catania and consisting of a total of 216 Si-CsI(Tl) telescopes, were set up at distances between 0.6 m and 1.1 m from the target. Their angular resolution and granularity were optimized in order to permit the identification of excited particle-unstable resonances in light fragments from the correlated detection of their decay products. For the measurements at the lower energies, the hodoscopes were mounted in the forward hemisphere in order to cover the angular region close to 90^0 in the center-of-mass system. At 1 GeV per nucleon, the hodoscopes were moved to the backward hemisphere in order to avoid the excessive background created by high-energetic δ electrons. A set of seven telescopes, each consisting of three Si detectors with thicknesses 50 μm, 300 μm, and 1000 μm, followed by a 4 cm long CsI detector, were mounted at selected angles. They served to simultaneously measure the yields of isotopically resolved light fragments.

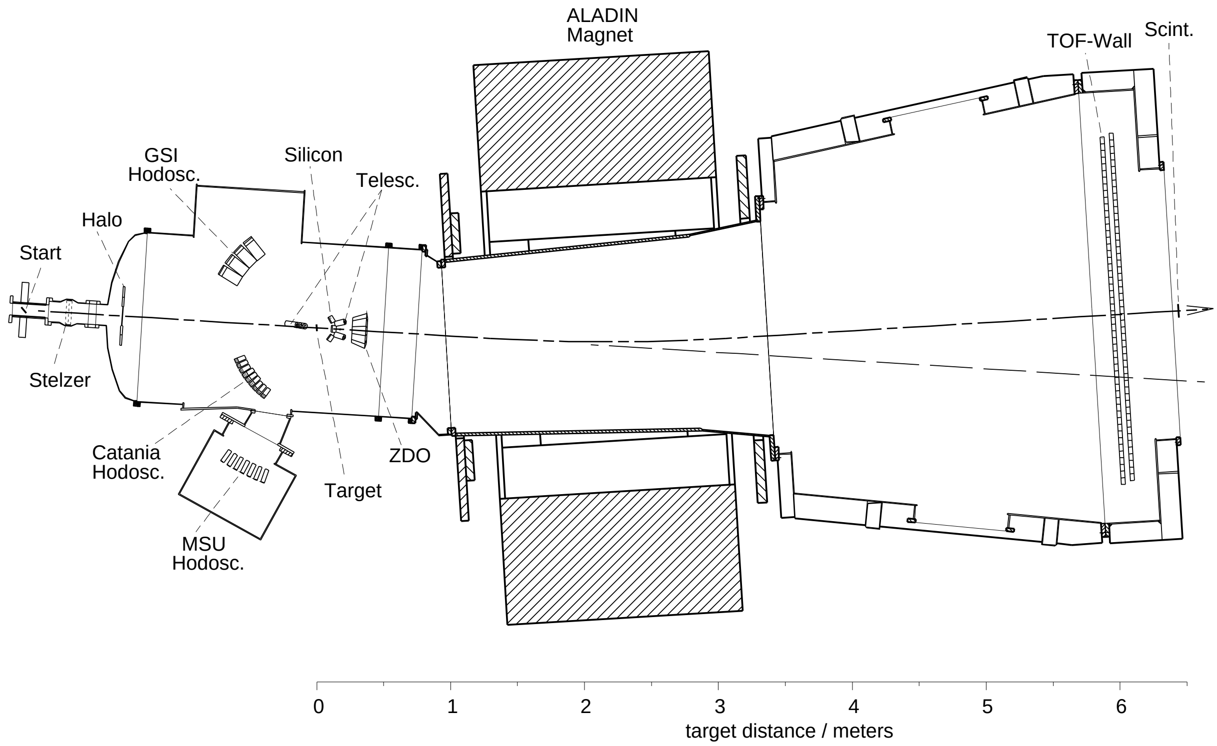

Figure 1: Schematic view of the experimental setup at the ALADIN spectrometer for the measurement with Au beams of 1 GeV per nucleon.

At 1 GeV per nucleon, impact-parameter selection was achieved by measuring, in coincidence, the quantity Z_{bound} for the projectile spectator with the time-of-flight wall of the ALADIN spectrometer. Z_{bound} is defined as the sum of the atomic numbers Z of all fragments with $Z \geq 2$ [18]. The hodoscopes are set up for the detection and identification of fragments emitted by the target spectator. The method used for impact parameter selection, therefore, exploits the symmetry of the collision system. At the same time, this method avoids autocorrelations of the impact parameter selection with the temperature measurement. At the lower bombarding energies, the associated charged particle multiplicity was sampled with a set of 36 CaF_2-plastic telescopes of the phoswich type, arranged symmetrically around the beam axis, and a set of 6 Si-strip detectors which, in total, represented 84 channels for charged-particle detection.

Temperature determination

The off-line analysis for the determination of temperatures from the yields of particle-unstable excited states consists of three parts:

a) the calibration of the more than 200 detectors,

b) the extraction of the resonance yields from the coincidence spectra, and

c) the determination of the acceptance values of the hodoscopes for each of these resonances.

The calibration is presently near completion. It is based on measurements with α and γ sources, on the observed punch-through points, and on the correlation of the responses of the Si and CsI detectors to particles of known identity and energy.

The coincidence spectra (plotted as a function of the relative momentum of the two coincident fragments) exhibit peaks due to resonance decay superimposed on the background of coincident but uncorrelated particle emission. In order to determine the background spectrum the technique of correlation functions is used. Correlation functions are created by dividing the coincidence yields by uncorrelated yields obtained from event-mixing. This eliminates a major part of non-interesting correlations, e.g. due to detector properties, which permits a more reliable estimate of the background.

Experimental correlation functions for p - α and d - ^{3}He coincidences, for the reaction Au + Au at 150 MeV per nucleon, are shown on the cover page. Both correspond to decay channels of ^{5}Li fragments, and the peaks due to the ground and excited (16.7 MeV) states are clearly visible. The solid lines represent the estimated background which, at large q, is close to one and, at small q, decreases due to the mutual Coulomb repulsion of the two charged particles. The background correlation function was determined with the aid of model calculations and by comparing to the correlation functions of other pairs of particles which are free of resonances in the region of small relative momenta, e.g. d + d.

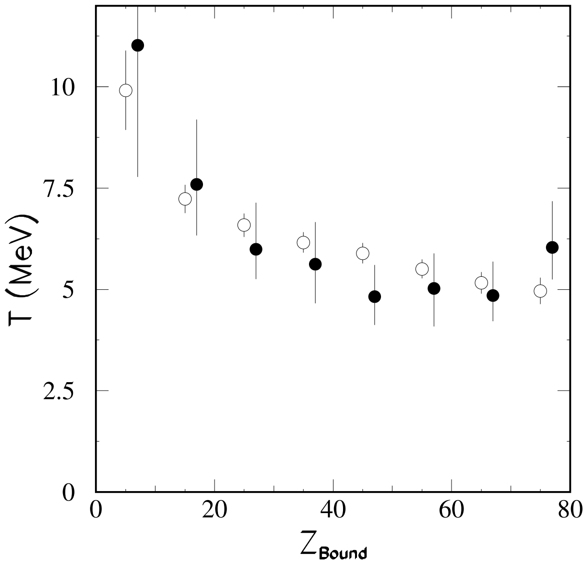

Figure 2: Temperatures extracted from the $(^3He/^4He)$ / $(^6Li/^7Li)$ double ratio of the Au+Au reaction at 1 GeV/nucleon are shown (open symbols) as a function of Z_{Bound}. They are in good agreement with the values obtained in the the previous experiment shown as closed symbols.

The acceptance of the hodoscopes for a particular resonance decay depends on the properties of the resonance and on the geometry and resolutions of the detectors. Monte-Carlo simulations are best suited for the determination of the socalled efficiency matrix. The modelling of additional effects such as multiple scattering in the target and in the detectors can easily be incorporated. The simulations also permit an assessment of the achieved experimental resolution and of the main factors contributing to it.

From the acceptance corrected yields the nuclear temperatures may then be calculated via:

$$\frac{Y_1}{Y_2} = \frac{2J_1 + 1}{2J_2 + 1}\, e^{-\Delta E/T}.$$

Here, Y_i, J_i are the yields and the spins of two states in the same isotope, e.g. the two states in ^{5}Li, separated by the energy ΔE. This assumes that the states of the decaying fragments are populated according to a Boltzmann law.

An additional complication is caused by the fact that the experimentally determined fragment yields may contain components due to the sequential decay of heavier fragments. This may require additional corrections. Model calculations show, however, that the case of the proton rich nucleus ^{5}Li is particularly favourable; the distortion by sequential feeding is predicted to be small. Clearly, it will be necessary to test this assumption and, more generally, to verify the assumption of a statistical population by attempting a consistent description of all observed resonance yields on the basis of sequential feeding models [10, 19, 20, 21, 22]. At the moment, the assumptions made in these models are quite crude and need some improvement.

While all these simulations are still in progress we could already extract temperatures from the double ratios of isotopic yields, measured with the four-element telescopes. The temperatures extracted from the (^{3}He/^{4}He) / (^{6}Li/^{7}Li) double ratio of the Au+Au reaction at 1 GeV/nucleon are shown in Fig. 2 (open symbols) as a function of Z_{Bound}. They are in good agreement with the values obtained in the the previous experiment (Au+Au at 1 GeV/nucleon, shown in Fig. 2 as closed symbols[23]). The observed agreement between the two measurements, therefore, mainly represents a methodical test. A major difference between the two experiments consists in the very different detection thresholds and in the different roles of the detector noise for the particle identification.

The Influence of Radial Flow on p-p Correlations

For an ideal, adiabatic expansion process, a simultaneous measurement of the freeze-out temperature and the degree of initial thermalization of the available center-of-mass energy is sufficient to determine the freeze-out density [16]. In general, however, the sharing of the available energy between collective radial motion and random (thermal) energy will also reflect the degree of dissipation during the expansion. Further constraints on the space-time density of the system at freeze-out might be provided by particle interferometry. Thus a combination of interferometric and thermodynamic informations might allow a closer look at the expansion dynamics.

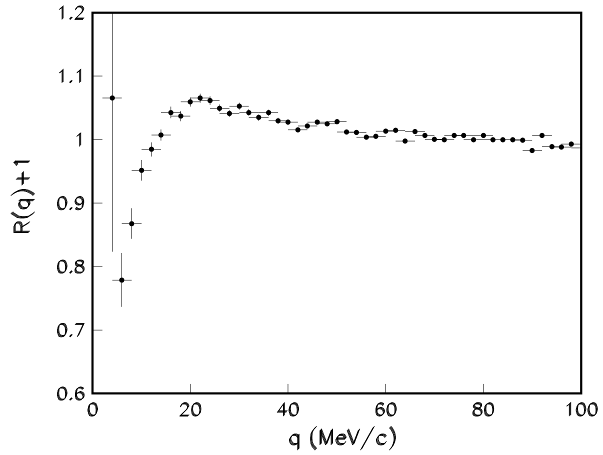

Figure 3: Proton - proton correlation for central ^{197}Au+^{197}Au collisions at E/A = 150 MeV.

Figure 3 shows a proton-proton correlation function R(q)+1 for central ^{197}Au+^{197}Au collisions measured at an incident beam energy of 150 MeV per nucleon. Here q denotes the momentum of relative motion. In order to exclude peripheral collisions where a heavy projectile fragment survives and to enhance more central collisions, limits of $Z_{bound} \leq 15$ and of a particle multiplicity in the Zero-Degree-Hodoscope (ZDO) and the silicon-strip detectors of ≥ 15 were required. The uncorrelated background was generated by event mixing and normalized to the coincident yield at large relative momenta q $\geq 150 MeV/c$.

Different from measurements with light projectiles in the Fermi-energy domain at beam energies below 100 MeV per nucleon, but similar to inclusive studies of the $^{40}Ar+^{197}Au$ reaction at 200 MeV per nucleon [12], one finds a rather weak correlation. Assuming, as a point of reference, a spherical Gaussian-shaped source of density $\rho(r) \propto e^{-r^2/r_0^2}$ and negligible lifetime [24],

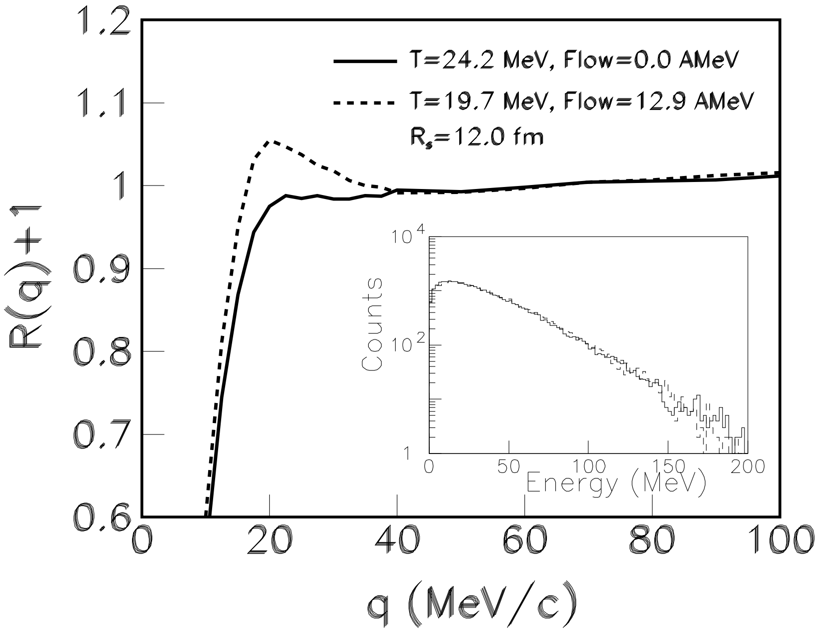

Figure 4: Calculated proton - proton correlation for two different combinations of random (thermal) and collective (flow) motion. The corresponding center-of-mass kinetic energy spectra are shown in the insert.

the observed strength is consistent with a source radius $r_0 \approx 6$ fm [25]. This value corresponds to a sharp sphere radius of $\mathrm{R}_s = \sqrt{5/2}r_0 \approx 10$ fm. While this theoretical estimate neglects correlations between momentum and ordinary space, a radial flow will introduce such correlations. Indeed, the analysis of the kinetic energy spectra of fragments in central Au+Au reactions has revealed a considerable collective outward motion superimposed on the random motion. At the breakup stage up to one-half of the energy available in the center-of-mass frame is stored in an explosive radial flow. This feature prevails, with monotonously increasing flow values, over the range of bombarding energies up to 1000 MeV per nucleon [14, 15, 17, 26]. For such large radial flow velocities, particle pairs at small relative momenta will probe only a limited spatial region of the source [27, 28], giving rise to smaller apparent source sizes.

In order to test the sensitivity of the proton-proton correlation to a collective expansion, schematic calculations based on the Pratt formalism [29, 30, 31] were performed. Nucleons were assumed to be emitted from a homogeneously filled sphere of radius R_s. In addition to the thermal velocity distribution characterized by a temperature parameter T, a self-similar flow profile was superimposed. Parameter pairs of the flow energy per nucleon at the surface, $(E/A)_f$, and the associated temperature parameter T were constrained to give (nearly) identical kinetic energy spectra which mimic the experimentally observed single proton spectra. The ambiguity in the parameters $(E/A)_f$ and T is illustrated in the insert in Fig. 4. There, the center-of-mass kinetic energy distribution for the case with no flow (T=24.2 MeV) is compared to the spectrum for $(E/A)_f$=12.9 MeV and T=19.7 MeV. Despite identical spatial source dimensions of R_s =12 fm, we obtain significantly enhanced *two*-particle correlation functions in the presence of flow (Fig. 4).

The apparent source radius is monotonously decreasing with increasing flow energy per nucleon, while for a given flow energy per nucleon the relative reduction is rather insensitive to the actual source radius (Fig. 5). For flow values comparable to the experimental findings in central

Au+Au collisions at E/A=150 MeV [15], we expect an apparent reduction of the source radius by approximately 15%. This leads to an overestimation of the density by about 40% if the effect of flow on the correlation function is neglected.

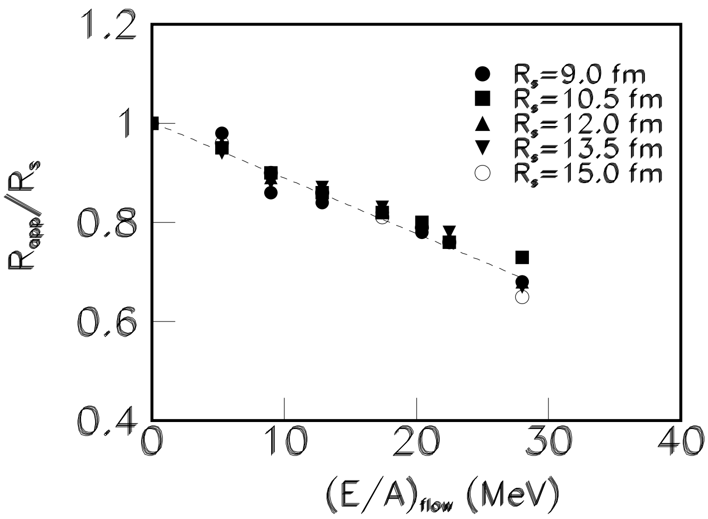

Figure 5: Apparent reduction of the relative source radius due to a collective radial flow. The calculation were performed for sharp sphere radii between 9 and 15 fm.

Clearly these considerations are still preliminary and schematic. Several other effects (e.g. finite lifetime, sequential decay, medium corrections to the p - p interaction, and multi-body Coulomb interactions) have to be considered in addition before definite conclusions can be reached. Nonetheless the present calculations illustrate that two particle correlations at small relative momenta show sensitivities to the expansion dynamics which are different from that of single-particle distributions. Therefore, these data, combined with detailed informations on the one-particle energy distributions of complex fragments, the isotopic distributions, and the relative population of excited states (see previous section) might enable a more detailed exploration of the break-up process.

Charge-Pickup of ^{238}U at Relativistic Energies

The process of charge-pickup by relativistic projectiles has been observed in numerous experiments. Projectiles between carbon and uranium have been studied in the energy regime of E/A = 0.5 to 2 GeV. With light projectiles, such as C, O, or Ne, cross sections below 1 mb were observed but, for heavier projectile nuclei, cross sections on the order of tens of mb have been measured. Systematic studies reported a quadratic dependence of the cross sections on the mass of the projectile [32]. A recent compilation has been given by Nilsen *et al.* [33]. With the availability of gold beams from the Brookhaven National Laboratory Alternating Gradient Synchrontron (AGS) results on charge-exchange processes at E/A $\approx$ 11 GeV were reported by various groups [33, 34, 35, 36]. A weak dependence on the mass of the target nuclei (hydrogen to lead) was found. Furthermore, the extracted excitation functions show a significant decrease of the cross sections as the energy increases.

Recently Sümmerer *et al.* measured a complete experimental isotope distribution of Cs products formed in the charge-exchange reaction ^{129}Xe incident on an Al target at 790 MeV/nucleon [37]. The large cross sections for neutron deficient isotopes indicated a dominant contribution from evaporation during the formation of the final Cs fragments. Furthermore, it was shown that intranuclear-cascade-plus-evaporation calculations can reproduce the observed yields for charge-pickup and the known strong increase of the cross section as a function of the mass of the projectile

[32]. According to the calculations, the cross section of the prefragment production increases approximately linearly with the mass of the projectile but the evaporation of protons depletes these yields and leads to the observed lower cross sections, especially for small neutron-deficient nuclei [37]. Experimental studies of the charge-pickup process for the heaviest projectiles available allow for further tests of the prediction that the cross sections should deviate significantly from the A^2-dependence observed for light and intermediate projectiles. Therefore, an extension of the existing systematics beyond $A_{proj} = 200$ was the main motivation of the present work to study charge-pickup of ^{238}U projectiles.

Charge-pickup of uranium at E/A = 960 MeV was investigated by Westphal *et al.* [38] who used a track-etch detector with high sensitivity. Not a single neptunium track ($Z = 93$) was found which led to an upper limit of 8 mb for the production cross section. It was concluded that this was due to the high fissility of the actinide upon the deposition of a moderate excitation energy; 40 MeV were considered to be sufficient to ensure that more than 90% of the hot Np nuclei fission. This estimate is consistent with the observation of an apparent mean mass loss of 5 to 7 nucleons associated with the charge-pickup for heavy projectiles like gold and holmium [39, 40].

In the present experiment the ALADIN forward spectrometer [41] at the heavy-ion synchrotron SIS at GSI was used to investigate charge-pickup of uranium via fission of projectile-like nuclei. Seven different targets (Be, C, Al, Cu, In, Au, U) with thicknesses between 185 and 800 mg/cm^2 were bombarded with ^{238}U-projectiles at incident energies of E/A = 600 and 1000 MeV. The fission fragments of these relativistic projectiles were emitted into a cone of polar angles less than 3 degrees, with respect to the beam axis. The geometrical acceptance of the ALADIN spectrometer ($\pm$9.2 degrees in horizontal and $\pm$4.3 degrees in vertical direction) was sufficient to detect both fission fragments simultaneously. The atomic numbers, positions, and angles of projectile fragments were measured with the ionization chamber MUSIC positioned behind the dipole magnet ALADIN. A description of the experimental setup can be found in Ref. [42]. With this setup a resolution of 0.6 (FWHM) was achieved for the sum charge of fission fragments (see Fig. 6).

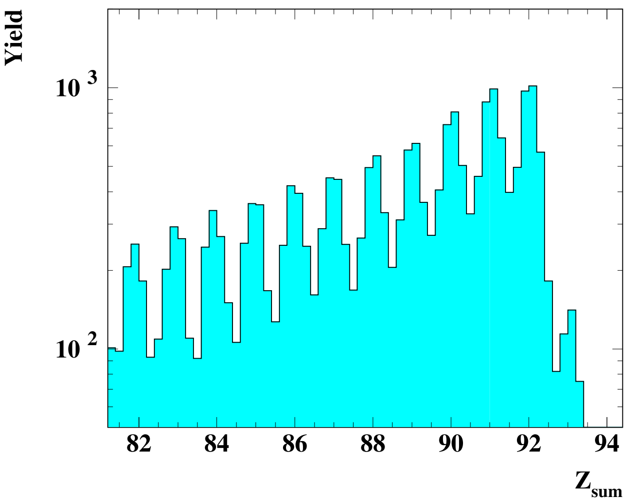

Figure 6: Spectrum of the sum charge Z_{sum} of fission fragments from the reactions ^{238}U on Al at E/A = 1000 MeV.

For the study of charge-pickup processes of uranium, events with a sum charge of 93 were selected. The experimental cross sections had to be corrected for nuclear interactions of the fission fragments in the target and in the materials of the detectors. To determine this effect, experimental total charge changing cross sections for various systems were used [43, 44, 45] and interpolations for typical fission fragments were made. Differences to calculated total reaction cross sections were used as an estimate of the associated uncertainty. Due to the finite double-hit resolution in the MUSIC the detection efficiency was limited to 87% at E/A = 600 MeV and 81% at E/A = 1000 MeV. The cross sections were corrected for this effect. The angular distribution of the fission fragments was assumed to be isotropic in the CM-system for the correction. This

Target	E/A 600 MeV $\sigma_{\Delta Z=+1}$ (mb)	E/A 1000 MeV $\sigma_{\Delta Z=+1}$ (mb)
Be	$61 \pm 3 \pm 4$	$27 \pm 2 \pm 2$
C	$77 \pm 2 \pm 5$	$36 \pm 2 \pm 3$
Al	$76 \pm 4 \pm 4$	$45 \pm 2 \pm 3$
Cu	$93 \pm 3 \pm 5$	$58 \pm 3 \pm 4$
In	$99 \pm 3 \pm 30$	$52 \pm 3 \pm 16$
Au	$186 \pm 9 \pm 19$	$64 \pm 3 \pm 12$
U	$151 \pm 4 \pm 17$	$99 \pm 6 \pm 22$

Table 1: Experimental cross sections for charge-pickup and subsequent fission of ^{238}U. Both the statistical (first values) and the systematical errors (second values) are given.

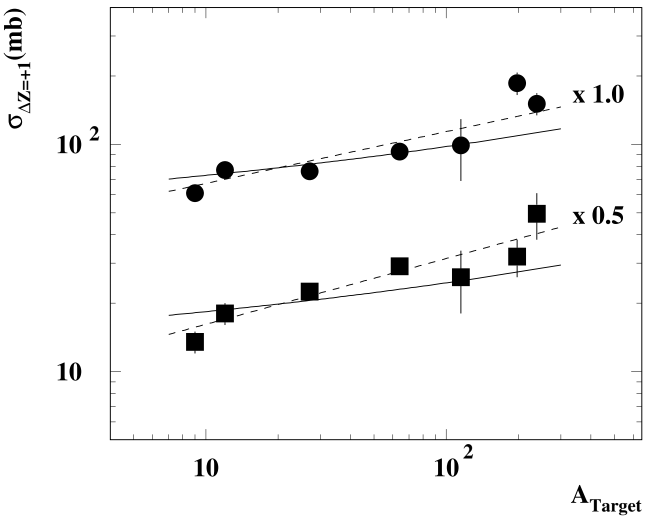

Figure 7: Cross sections for charge-pickup and subsequent fission of ^{238}U-projectiles at E/A = 600 (*dots*) and 1000 MeV (*squares*). The lines show power law fits (*dashed lines*) and fits to $A_t^{1/3} + A_p^{1/3} - 0.75(A_t^{-1/3} + A_p^{-1/3})$ (*full lines*). The error bars denote the statistical and systematic errors combined in quadrature.

assumption is, however, not crucial [42].

In Fig. 7 and Tab. 1 we show the experimental cross sections for charge-pickup of ^{238}U and subsequent fission as a function of the mass of the target. The dashed lines indicate power law fits to the data as suggested by Nilsen *et al.* [33] whereas the full lines show the results of a linear fit to $A_t^{1/3} + A_p^{1/3} - 0.75(A_t^{-1/3} + A_p^{-1/3})$ as it may be expected for peripheral nuclear collisions [46]. Due to the experimental uncertainties, especially for heavy targets, no decision can be made which of the parameterizations gives a better description of the data. In a later discussion we will show that nearly the full cross section for charge-pickup of ^{238}U can be found in the fission channel.

We should note that the dominant contribution to the systematic errors is due to the finite experimental charge resolution and the resulting overlap of the Z_{sum}=92 and 93 channels. As we have shown in a previous paper [42] the cross section for electromagnetic fission leading to $Z_{sum} = 92$ increases approximately quadratically with the charge of the target. Therefore the ratio of the yield with $Z_{sum} = 93$ to $Z_{sum} = 92$ decreases strongly as the charge number of the target increases.

Following the suggestion of Sümmerer *et al.* [37], intranuclear-cascade-plus-evaporation calculations were performed using the code ISAPACE [47, 48, 49]. At relativistic energies and very peripheral collisions, intranuclear-cascade (INC) calculations based on experimental free hadron-hadron cross sections were successful in describing experimental data, see e.g. Ref. [37, 50]. The INC code ISABEL is, except for the quantum mechanical ingredient of the Pauli-blocking, a purely classical model and accounts for the diffuseness of the nuclear surface. Nuclear charge exchange processes proceed in the model either via (n,p)-charge exchange collisions where a virtual charged pion is exchanged or by excitation of a Δ-resonance with subsequent emission of

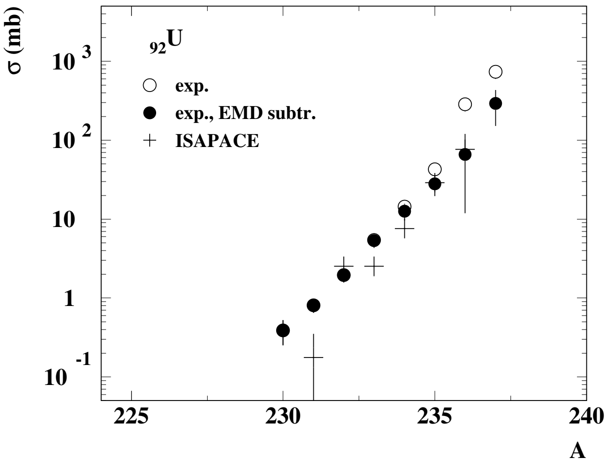

Figure 8: Experimental cross sections for the production of uranium isotopes in the reaction ^{238}U + ^{nat}Cu at E/A = 950 MeV (*open circles*, data from Ref. [51]). The nuclear part of the cross sections (*full circles*, obtained by subtracting the electromagnetic contribution) is compared to the results of ISAPACE calculations (*crosses*).

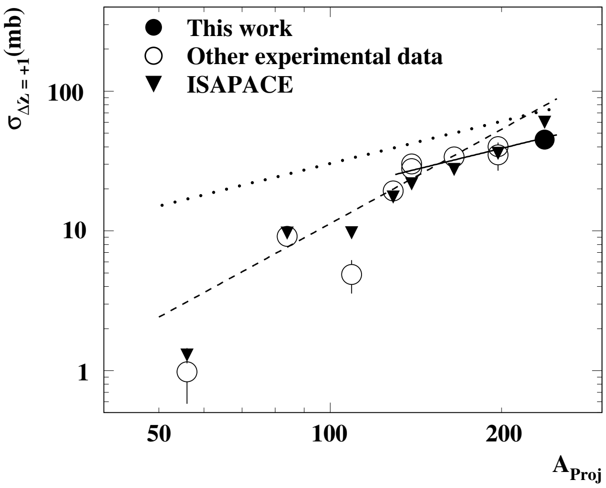

Figure 9: Experimental cross sections for charge-pickup as a function of the projectile mass from several measurements [33, 37, 39, 53, 54]. All data have been obtained by using an Al-target. Both quadratic (*dashed*) and linear (*full line*) dependences are shown. For comparison the results of ISAPACE calculations are shown (*triangles*). The dotted line shows the results from ISABEL calculations, prior to evaporation.

a negative pion. The excited prefragments decay subsequently by light particle emission or by fission. This de-excitation is modeled by the statistical evaporation code PACE. To verify the validity of this description for fission reactions in the energy regime of E/A = 1 GeV, we compared the calculated formation cross sections of uranium isotopes from the reaction ^{238}U + ^{nat}Cu at a bombarding energy of 950 MeV/nucleon with experimental results [51]. The data include contributions from electromagnetic neutron removal processes [52]. In Fig. 8 we show both the experimental data and the results of ISAPACE calculations. A good description is achieved after calculated electromagnetic contributions [42] are taken into account.

A reasonable agreement is obtained for the charge-exchange process leading to the formation of Np and subsequent fission in the reaction ^{238}U + Al at 600 and 1000 MeV/nucleon; ISAPACE calculations result in cross sections of 74±6 mb and 59±5 mb, respectively. In Fig. 9, we present a comparison of charge-pickup cross sections in the energy regime of E/A ≈ 1 GeV for different projectiles interacting with Al targets [33, 37, 39, 53, 54]. The experimental trend as a function of the mass of the projectile is correctly reproduced by ISAPACE calculations. We also show the results from ISABEL calculations, prior to evaporation. The production cross sections of prefragments with $\Delta Z=+1$ increases approximately linearly with the mass of the projectile. While the evaporation of neutrons does not change the cross sections, the evaporation of protons depletes the yields and lead to the formerly discussed lower cross sections, especially for light nuclei where the Coulomb barriers hinder the evaporation of protons less than in the case of heavy nuclei. Therefore, the survival probability with respect to light charged particle emission, increases from ~5% for iron to 80% in the case of uranium. Our results confirm the expected behavior [37] for the heaviest projectiles available.

An estimate of the excitation energy can be achieved from the number of evaporated neutrons. Our measurements of the fragments mass yield a broad distribution with a mean mass loss ΔA_{sum} of approximately 9 neutrons in total. After subtracting $\sim$ 3 postscission neutrons [55] it can be estimated that about 6 neutrons were evaporated during the de-excitation of the formed Np-nucleus. A comparable number of neutrons was found in other experiments using heavy projectiles like lanthanum, holmium and gold [39, 40]. Under the assumption that one neutron carries away 8 MeV, the total mass loss corresponds to a mean excitation energy of the prefragment going into the $\Delta Z = +1$ exit channel of roughly 50 MeV. This result is in good agreement with the experimental findings of Westphal *et al.* [40] and with ISAPACE calculations which predict a mean mass loss of $\sim$9 neutrons from the Np prefragment ($\overline{A_{pref}} = 237$) and a fission probability of $\sim$98%. Therefore, nearly the full pickup cross section is found in the fission channel.

In conclusion, we measured the charge-pickup cross sections for relativistic ^{238}U-projectiles by investigating the fission channel. Good agreement with intranuclear-cascade-plus-evaporation calculations is observed. As pointed out earlier by Sümmerer *et al.* [37], it is not necessary to invoke coherent processes to explain the observed cross sections for charge-pickup processes. Both experimental results and ISAPACE calculations show a mean mass loss for the fission fragments of approximately 9 neutrons in total caused by the de-excitation of the formed Np-nucleus and the additional evaporation of $\sim$3 fission neutrons. From the calculations it can be estimated that $\sim$78% of the prefragments fission and another 20% decay via light charged particle emission. The present results are, however, consistent with the nonobservation of Np-nuclei, reported in a previous publication [38].

The authors would like to thank K. Sümmerer for interesting and helpful discussions and for providing the ISAPACE code.

References

[1] *GSI Nachrichten 03-95, 1995.*

[2] J. Pochodzalla *et al.*, Phys. Rev. Letter **75**, 1040 (1995).

[3] G.J. Kunde *et al.*, Phys. Rev. Lett. **74**, 38 (1995).

[4] J. Bondorf *et al.*, Phys. Lett. B **359**, 261 (1995).

[5] L.G. Moretto, private communication.

[6] J.B. Natowitz *et al.*, Phys. Rev. C **52**, R2322 (1995).

[7] M.B. Tsang, *et al.*, Phys. Rev. C, in print.

[8] J. Pochodzalla *et al.*, Phys. Rev. C **35**, 1695 (1987).

[9] F. Saint-Laurent *et al.*, Phys. Lett. B **202**, 190 (1988).

[10] T.K. Nayak *et al.*, Phys. Rev. C **45**, 132 (1992).

[11] H. Xi *et al.*, Nucl. Phys. A **552**, 281 (1993).

[12] G.J. Kunde *et al.*, Phys. Rev. Lett. **70**, 2545 (1993).

[13] C. Schwarz *et al.*, Phys. Rev. C **48**, 676 (1993).

[14] W. Reisdorf *et al.*, in *Proceedings of the International Workshop XXII, Hirschegg, 1994.*

[15] S.C. Jeong *et al.*, Phys. Rev. Lett. **72**, 3468 (1994).

[16] G. Papp and W. Nörenberg, GSI-preprint GSI-95-30, 1995 (to be published).

[17] W.C. Hsi *et al.*, Phys. Rev. Lett. **73**, 3367 (1994).

[18] J. Hubele *et al.*, Z.Phys. A **340** 263 (1991).

[19] Z. Chen and C.K. Gelbke, Phys. Rev. C **38**, 2630 (1988).

[20] T.K. Nayak *et al.*, Phys. Rev. Lett. **62**, 1021 (1989).

[21] F. Zhu *et al.*, Phys. Lett. B **282**, 299 (1992).

[22] C. Schwarz *et al.*, Phys. Rev. C **49**, 3316 (1994).

[23] T. Möhlenkamp, PhD thesis, Frankfurt (1996), in preparation

[24] S.E. Koonin, Phys. Lett. **70B**, 43 (1977).

[25] Detector resolution effects are not yet taken into account in the calculations.

[26] W. Bauer *et al.*, Phys. Rev. C**47**, R1838 (1993).

[27] W.Q. Chao *et al.*, Phys. Rev. C **49**, 3224 (1994).

[28] S.V. Akkelin and Yu.M. Sinyukov, Phys. Lett. B **356**, 525 (1995).

[29] S. Pratt, Phys. Rev. Lett. **53**, 1219 (1984).

[30] S. Pratt and W. Bauer, in *Proc. CORINNE 90, International Workshop on Particle Correlations and Interferometry*, edt. D. Ardouin, Singapore: World Sci. (1990), p. 183.

[31] W.G. Gong *et al.*, Phys. Rev. Lett. **65**, 2114 (1990) and Phys. Rev. C **43**, 781 (1991).

[32] Ren Guoxiao *et al.*, Phys. Rev. C **39**, 1351 (1989).

[33] B.S. Nilsen *et al.*, Phys. Rev. C **50**, 1065 (1994).

[34] Y.D. He and P.B. Price, Phys. Lett. B **298**, 50 (1993)
Y.D. He, Ph.D. thesis, University of California at Berkeley, 1993.

[35] S.E. Hirzebruch *et al.*, Phys. Rev. C **51**, 2085 (1995).

[36] L.Y. Geer *et al.*, Phys. Rev. C **52**, 334 (1995).

[37] K. Sümmerer *et al.*, Phys. Rev. C **52**, 1106 (1995).

[38] A.J. Westphal *et al.*, Phys. Rev. C **45**, 2423 (1992).

[39] J.R. Cummings *et al.*, Phys. Rev. C **42**, 2508 (1990).

[40] A.J. Westphal *et al.*, Phys. Rev. C **44**, 1687 (1991).

[41] J. Hubele *et al.*, Z. Phys. A **340**, 263 (1991).

[42] Th. Rubehn *et al.*, Z. Phys. A **353**, 197 (1995).

[43] W.R. Binns *et al.*, Phys. Rev. C **36**, 1870 (1987).

[44] W.R. Webber *et al.*, Phys. Rev. C **41**, 520 (1990).

[45] Y.D. He and P.B. Price, Z. Phys. A **348**, 105 (1994).

[46] C.J. Benesh, B.C. Cook, and J.P. Vary, Phys. Rev. C **40**, 1198 (1989).

[47] Y. Yariv and Z. Fraenkel, Phys. Rev. C **20**, 2227 (1979).

[48] T. Blaich *et al.*, Phys. Rev. C **45**, 689 (1992).

[49] K.-H. Schmidt *et al.*, Nucl. Phys. A **542**, 699 (1992).

[50] K. Sümmerer *et al.*, Phys. Rev. C **42**, 2546 (1990).

[51] H.-G. Clerc *et al.*, Nucl. Phys. A **590**, 785 (1995).

[52] T. Aumann *et al.*, Z. Phys. A **352**, 163 (1995).

[53] G. Gerbier, Ren Guoxiao, and P.B. Price, Phys. Rev. Lett. **60**, 2258 (1988).

[54] W.R. Binns *et al.*, Phys. Rev. C **39**, 1785 (1989).

[55] C. Wagemans, *The Nuclear Fission Process* (CRC Press, Boca Raton - Ann Arbor - Boston - London, 1991).

C. Schwarz,[(1)] 郗鸿飞 Hongfei Xi,[(1)] and Th. Rubehn,[(1)*] for the ALADIN collaboration:

M. Begemann-Blaich,[(1)] Th. Blaich,[(2)] A. Ferrero,[(3)†] S. Fritz,[(1)] C. Groß,[(1)] G. Immé,[(4)] I. Iori,[(3)] U. Kleinevoß,[(1)] G.J. Kunde,[(1)‡] W.D. Kunze,[(1)] V. Lindenstruth,[(1)§] U. Lynen,[(1)] M. Mahi,[(1)] T. Möhlenkamp,[(5)] A. Moroni,[(3)] W.F.J. Müller,[(1)] B. Ocker,[(6)] T. Odeh,[(1)] J. Pochodzalla,[(1)] G. Raciti,[(4)] H. Sann,[(1)] M. Schnittker,[(1)] A. Schüttauf,[(6)] W. Seidel,[(5)] V. Serfling,[(6)] W. Trautmann,[(1)] A. Trzcinski,[(7)] A. Tucholski,[(7)] G. Verde,[(4)] A. Wörner,[(1)] E. Zude,[(1)] B. Zwieglinski[(7)]

[(1)]Gesellschaft für Schwerionenforschung, 64220 Darmstadt, Germany
[(2)]Institut für Kernchemie, Universität Mainz, 55099 Mainz, Germany
[(3)]Dipartimento di Fisica, Università di Milano and I.N.F.N., 20133 Milano, Italy
[(4)]Dipartimento di Fisica dell' Università and I.N.F.N., 95129 Catania, Italy
[(5)]Forschungszentrum Rossendorf, 01314 Dresden, Germany
[(6)]Institut für Kernphysik, Universität Frankfurt, 60486 Frankfurt, Germany
[(7)]Soltan Institute for Nuclear Studies, 00 681 Warsaw, Hoza 69, Poland

J.P. and M.B. acknowledge the financial support of the Deutsche Forschungsgemeinschaft under the Contract No. Po256/2-1 and Be1634/1-1, respectively. This work was supported in part by the European Community under contract ERBCHGE-CT92-0003 and ERBCIPD-CT94-0091.

[*]Present address: Lawrence Berkeley Laboratory, Berkeley, CA 94720
[†]On leave from the Comision Nacional Energia Atomica, Argentina
[‡]Present address: MSU-NSCL, East Lansing, MI 48824, USA
[§]Present address: Lawrence Berkeley Laboratory, Berkeley, CA 94720